

⁷⁹Br, ¹²⁷I NQR of Diammoniumalkyl Halides and Piperazinium Halides.

Crystal Structure of Piperazinium Dibromide Monohydrate and Piperazinium Monoiodide

Jutta Hartmann*, Shi-Qi Dou, and Alarich Weiss

Institut für Physikalische Chemie, Physikalische Chemie III, Technische Hochschule, Darmstadt, West Germany

Z. Naturforsch. **44a**, 41–55 (1989); received October 22, 1988

The ⁷⁹Br and ¹²⁷I NQR spectra were investigated for 1,2-diammoniummethane dibromide, -diiodide, 1,3-diammoniumpropane dibromide, -diiodide, piperazinium dibromide monohydrate, and piperazinium monoiodide in the temperature range $77 \leq T/\text{K} \leq 420$. Phase transitions could be observed for the three iodides. The temperatures for the phase transitions are: 400 K and 404 K for 1,2-diammoniummethane diiodide, 366 K for 1,3-diammoniumpropane diiodide, and 196 K for piperazinium monoiodide.

The crystal structures were determined for the piperazinium compounds. Piperazinium dibromide monohydrate crystallizes monoclinic, space group $C2/c$, with $a = 1148.7$ pm, $b = 590.5$ pm, $c = 1501.6$ pm, $\beta = 118.18^\circ$, and $Z = 4$. For piperazinium monoiodide the orthorhombic space group $Pmn2_1$ was found with $a = 958.1$ pm, $b = 776.9$ pm, $c = 989.3$ pm, $Z = 4$. Hydrogen bonds $N-H \dots X$ with $X = \text{Br}, \text{I}$ were compared with literature data.

Introduction

Recently we have studied the nuclear quadrupole resonance (NQR) spectra of halogen ions (⁷⁹Br and ¹²⁷I) in several toluidinium and paraphenylenediammonium halides [1]. $[1,4-(\text{H}_3\text{N})_2\text{C}_6\text{H}_4]^{2+} \cdot [\text{I}]_2^{2-}$, paraphenylenediammonium diiodide, is an interesting substance. At $T = 139$ K a phase transition occurs, which is most probably of higher order than 1. By passing the transition temperature, the symmetry of the solid is lowered. In the high temperature phase, phase I, stable at $T > T_c = 139$ K, the point symmetry of the iodide ions in the lattice must be tetragonal or higher because the asymmetry parameter of the electric field gradient tensor, $\eta(^{127}\text{I}) = |\Phi_{xx} - \Phi_{yy}|/|\Phi_{zz}|$ is zero. Below T_c , in the low temperature phase II, $\eta(^{127}\text{I})$ becomes non-zero, proving the lowering of the site symmetry of the iodine atoms in the lattice. Preliminary X-ray work shows that the unit cell of the high temperature phase I is tetragonal, with $Z = 2$ formula units in the unit cell. From the information gained on anilinium bromide and anilinium iodide

[2–8], it is assumed that the phase transition is connected with the dynamics of the $-\text{NH}_3$ group in the solid.

It seemed to be of interest to study diammonium-alkyl halides $[\text{H}_3\text{N}(\text{CH}_2)_n\text{NH}_3]^{2+} \cdot 2\text{X}^-$, $\text{X} = \text{Br}, \text{I}$, and hydrohalides of cyclic non-aromatic diamines in order to observe there the possible onset of dynamic order-disorder of the hydrogen bond system $-\text{N}-\text{H} \dots \text{X}$. In the following we report on ⁷⁹Br and ¹²⁷I NQR studies of: 1,2-diammoniummethane dibromide, $\text{C}_2\text{H}_{10}\text{Br}_2\text{N}_2$; 1,2-diammoniummethane diiodide, $\text{C}_2\text{H}_{10}\text{I}_2\text{N}_2$; 1,3-diammoniumpropane dibromide, $\text{C}_3\text{H}_{12}\text{Br}_2\text{N}_2$; 1,3-diammoniumpropane diiodide, $\text{C}_3\text{H}_{12}\text{I}_2\text{N}_2$; piperazinium dibromide monohydrate, $\text{C}_4\text{H}_{14}\text{Br}_2\text{N}_2\text{O}$; piperazinium monoiodide, $\text{C}_4\text{H}_{11}\text{IN}_2$. The crystal structure of the later two compounds is reported, too.

Experimental

Preparation, Chemical Analysis

The compounds were prepared by mixing stoichiometric portions of the amines, dissolved in H_2O (or mixtures of $\text{H}_2\text{O}/\text{C}_2\text{H}_5\text{OH}$), and diluted aqueous HBr and HI, respectively. The compounds were crystallized from the solutions either by cooling or by evapo-

Reprint requests to Prof. Dr. Al. Weiss, Institut für Physikalische Chemie, Technische Hochschule Darmstadt, Petersenstraße 20, D-6100 Darmstadt.

* Part of the Dr.-Ing. Dissertation of Jutta Hartmann, D 17, Technische Hochschule Darmstadt.

0932-0784 / 89 / 0100-0041 \$ 01.30/0. – Please order a reprint rather than making your own copy.



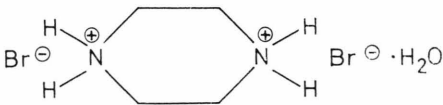
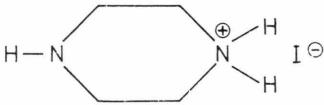
Dieses Werk wurde im Jahr 2013 vom Verlag Zeitschrift für Naturforschung in Zusammenarbeit mit der Max-Planck-Gesellschaft zur Förderung der Wissenschaften e.V. digitalisiert und unter folgender Lizenz veröffentlicht: Creative Commons Namensnennung-Keine Bearbeitung 3.0 Deutschland Lizenz.

Zum 01.01.2015 ist eine Anpassung der Lizenzbedingungen (Entfall der Creative Commons Lizenzbedingung „Keine Bearbeitung“) beabsichtigt, um eine Nachnutzung auch im Rahmen zukünftiger wissenschaftlicher Nutzungsformen zu ermöglichen.

This work has been digitalized and published in 2013 by Verlag Zeitschrift für Naturforschung in cooperation with the Max Planck Society for the Advancement of Science under a Creative Commons Attribution-NoDerivs 3.0 Germany License.

On 01.01.2015 it is planned to change the License Conditions (the removal of the Creative Commons License condition “no derivative works”). This is to allow reuse in the area of future scientific usage.

Table 1. Characterization of the compounds studied. Chemical analysis (in weight%). (^a Decomposition.)

Compound	Color/Habitus	Mp/K	Chemical analysis							
			C		H		N		Br(I)	
			exp.	calc.	exp.	calc.	exp.	calc.	exp.	calc.
1,2-Diammoniummethane dibromide $[\text{H}_3\text{N}(\text{CH}_2)_2\text{NH}_3]^{2+} \cdot 2 \text{Br}^-$	white plates	623 ^a	10.70	10.82	4.38	4.54	12.67	12.62	71.97	72.01
1,2-Diammoniummethane diiodide $[\text{H}_3\text{N}(\text{CH}_2)_2\text{NH}_3]^{2+} \cdot 2 \text{I}^-$	white plates	588 ^a	7.57	7.60	3.02	3.19	8.92	8.86	79.29	80.34
1,3-Diammoniumpropane dibromide $[\text{H}_3\text{N}(\text{CH}_2)_3\text{NH}_3]^{2+} \cdot 2 \text{Br}^-$	white needles	523 ^a	15.24	15.27	5.08	5.12	11.94	11.87	67.54	67.73
1,3-Diammoniumpropane diiodide $[\text{H}_3\text{N}(\text{CH}_2)_3\text{NH}_3]^{2+} \cdot 2 \text{I}^-$	light yellow needles	530 ^a	10.89	10.92	3.58	3.66	8.57	8.49	76.95	76.92
Piperazinium dibromide monohydrate	white needles	595 ^a	17.90	18.01	5.39	5.29	10.35	10.50	59.62	59.92
										
Piperazinium monoiodide	clear crystal	517	22.53	22.45	5.38	5.18	13.08	13.09	59.67	59.29
										

ration of the solvent. The solids, gained this way, were analysed (C, N, H, Br, I). If necessary, they were recrystallized from H_2O . The results of the preparation and the chemical analysis are listed in Table 1.

Crystal Structure Determination

Small crystals of piperazinium dibromide monohydrate and of piperazinium monoiodide were grown for single crystal diffractometry from solution in mixtures $\text{C}_2\text{H}_5\text{OH}/\text{H}_2\text{O}$ and methanolic solution, respectively, by evaporation of the solvent. X-ray diffraction intensity data were collected on a four circle goniometer (MoK α radiation). By use of direct methods the crystal structures were determined and refined by least squares procedure.

^{79}Br and ^{127}I Nuclear Quadrupole Resonance

Polycrystalline samples of the compounds studied were investigated by use of a NQR spectrometer

working in the superregenerative mode with sideband suppression and magnetic modulation. The following frequency ranges were covered to search for the resonance frequencies: 1,2-diammoniummethane dibromide, 12.5 MHz–20 MHz; 1,2-diammoniummethane diiodide, 14 MHz–34 MHz; 1,3-diammoniumpropane dibromide, 11.5 MHz–23.1 MHz; 1,3-diammoniumpropane diiodide, 7 MHz–40 MHz; piperazinium dibromide monohydrate, 12 MHz–23.1 MHz; piperazinium monoiodide, 11 MHz–43.5 MHz. For the bromides studied, the frequency range covered was selected wide enough to observe in every case the ^{81}Br NQR frequencies corresponding to the ^{79}Br NQR spectrum. They have been observed and the ratio $\nu(^{79}\text{Br})/\nu(^{81}\text{Br}) = Q(^{79}\text{Br})/Q(^{81}\text{Br}) = 1.197$ was found. For measurements of the temperature dependence of the NQR spectra, the appropriate sample temperatures were generated via thermostats (temperature range and estimated error in T , method): $300 \leq (T \pm 0.5)/\text{K} \leq 420$, oil thermostat; $200 \leq (T \pm 0.3)/\text{K}$

	Piperazinium dibromide monohydrate	Piperazinium monoiodide
Crystal habitus, size	colorless needle (0.15 × 0.15 × 1.0) mm ³	flat prism (0.14 × 0.27 × 0.75) mm ³
Diffractionmeter		Stoe-Stadi-4
Wavelength/pm (Mo–K α)		71.069
Monochromator		Graphit (002)
Temperature/K	297	299
Absorption coefficient (μ/m^{-1})	8782	4201
Scan		$\omega/2\theta$
($\sin \theta/\lambda$) _{max} /pm	0.00756	0.0065
Number of measured reflexions	6196	1784
Symmetry independent reflexions	1620	942
Reflexions considered	1572	941
Number of free parameters	67	109
$F(000)$	520	477
$R(F)$	0.048	0.022
$R_w(F)$	0.039	0.019
Lattice constants		
a/pm	1148.7(3)	958.1(3)
b/pm	590.5(2)	776.9(2)
c/pm	1501.6(3)	989.3(3)
$\beta/^\circ$	118.18(1)	
Volume of the unit cell $V \cdot 10^{-6}/(\text{pm})^3$	897.82	736.38
Space group	$C2/c-C_{2h}^6$	$Pmn2_1-C_{2v}^7$
Formula units per unit cell	4	4
$\rho_{\text{calc}}/\text{Mg} \cdot \text{m}^{-3}$	1.97 ($T = 297\text{ K}$)	1.93 ($T = 299\text{ K}$)
$\rho_{\text{pykn}}/\text{Mg} \cdot \text{m}^{-3}$	1.95 ($T = 295\text{ K}$)	1.92 ($T = 295\text{ K}$)
Point positions	O in 4e: 0, y , 1/4; 0, \bar{y} , 3/4 all others in 8f: x , y , z ; \bar{x} , \bar{y} , \bar{z} ; \bar{x} , y , 1/2 – z ; x , \bar{y} , 1/2 + z	I, N, H ^(N) in 2a: 0, y , z ; 1/2, \bar{y} , 1/2 + z all others in 4b: x , y , z ; \bar{x} , y , z ; 1/2 – x , \bar{y} , 1/2 + z ; 1/2 + x , \bar{y} , 1/2 + z

Table 2. Experimental conditions for the structure determination of piperazinium dibromide monohydrate $\text{C}_4\text{H}_{14}\text{Br}_2\text{N}_2\text{O}$ and piperazinium monoiodide $\text{C}_4\text{H}_{11}\text{IN}_2$. Crystallographic data are given, too.

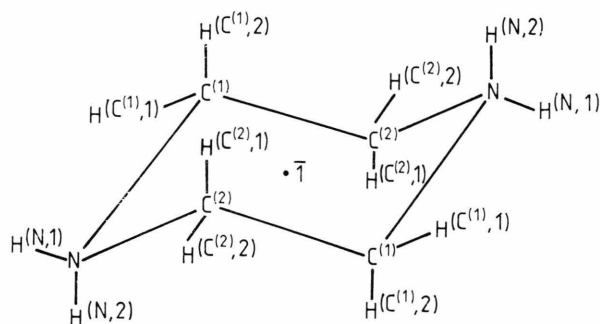


Fig. 1. Sketch of the di-cation $[\text{C}_4\text{H}_{12}\text{N}_2]^{2+}$ of piperazinium dibromide monohydrate.

$\pm 0.005\text{ MHz}$; this limitation is due to the NQR line width.

Results

Crystal Structures

In Table 2 we have listed the experimental conditions under which the structure determinations of the piperazinium compounds have been performed. Also given are the space groups, lattice constants, and mass densities. The positional and thermal parameters found for piperazinium dibromide monohydrate, $\text{C}_4\text{H}_{14}\text{Br}_2\text{N}_2\text{O}$, are listed in Table 3; Table 4 gives these parameters for the compound piperazinium monoiodide, $\text{C}_4\text{H}_{11}\text{IN}_2$. The intramolecular distances and angles for the piperazinium di-cation, $[\text{C}_4\text{H}_{12}\text{N}_2]^{2+}$, are given in Table 5. Note that this ca-

≤ 300 , methanol thermostat; $120 \leq (T \pm 0.8)/\text{K} \leq 200$, thermostated nitrogen gas stream; $(77 \pm 0.3)\text{ K}$, liquid nitrogen bath. The temperature at the sample site was measured via a copper-constantan thermocouple. The frequencies determined are accurate to

Table 3. Positional and thermal parameters of piperazinium dibromide monohydrate $\text{C}_4\text{H}_{14}\text{Br}_2\text{N}_2\text{O}$. The temperature factor is of the form $T = \exp\{-2\pi^2(U_{11}h^2a^{*2} + U_{22}k^2b^{*2} + U_{33}l^2c^{*2} + 2U_{12}hka^*b^* + 2U_{13}hla^*c^* + 2U_{23}klb^*c^*)\}$. The U_{ij} are given in $(\text{pm})^2$; U is the isotropic mean for the hydrogen atoms. The errors are given in brackets.

Atom	x/a	y/b	z/c	U_{11}, U	U_{22}	U_{33}	U_{12}	U_{13}	U_{23}
O	0.0	0.3679 (6)	0.25	516(22)	429(19)	609(26)	0	229(20)	0
Br	0.2092 (0)	0.8336 (0)	0.3429 (0)	268 (2)	433 (2)	277 (2)	83(1)	105 (1)	6(1)
N	0.5216 (2)	0.4622 (4)	0.6013 (2)	277 (9)	337(11)	223 (9)	11(7)	116 (7)	1(8)
C ⁽¹⁾	0.5813 (2)	0.6651 (4)	0.4851 (2)	278(11)	318(11)	294(12)	-44(8)	135 (9)	-24(9)
C ⁽²⁾	0.5439 (3)	0.6906 (4)	0.5687 (2)	345(13)	289(12)	276(12)	-33(9)	138(10)	-61(9)
H ^{(C(1), 1)}	0.5904(45)	0.8308(64)	0.4623(42)	600					
H ^{(C(1), 2)}	0.6623(43)	0.5558(77)	0.5180(32)	600					
H ^{(C(2), 1)}	0.4602(46)	0.7691(85)	0.5477(37)	600					
H ^{(C(2), 2)}	0.6125(42)	0.7543(79)	0.6330(34)	600					
H ^(O)	0.0689(45)	0.4492(76)	0.2730(36)	600					
H ^(N, 1)	0.4964(44)	0.4913(67)	0.6526(36)	600					
H ^(N, 2)	0.5929(46)	0.3899(85)	0.6275(34)	600					

Table 4. Positional and thermal parameters of piperazinium monoiodide $\text{C}_4\text{H}_{11}\text{IN}_2$. The temperature factor is of the form $T = \{-2\pi^2(U_{11}h^2a^{*2} + U_{22}k^2b^{*2} + U_{33}l^2c^{*2} + 2U_{12}hka^*b^* + 2U_{13}hla^*c^* + 2U_{23}klb^*c^*)\}$. The U_{ij} are given in $(\text{pm})^2$; U is the isotropic mean for the hydrogen atoms. Errors are given in brackets.

Atom	x/a	y/b	z/c	U_{11}, U	U_{22}	U_{33}	U_{12}	U_{13}	U_{23}
I ⁽¹⁾	0.0	0.2013 (1)	0.0000 (1)	463 (2)	372 (2)	437 (3)	0	0	62 (2)
I ⁽²⁾	0.0	0.2705 (1)	0.4647 (1)	533 (3)	355 (2)	482 (3)	0	0	72 (2)
N ⁽¹⁾	0.0	0.7605 (9)	0.0889 (10)	724(55)	397(33)	238(43)	0	0	-60(29)
N ⁽²⁾	0.0	0.7272 (9)	0.3784 (11)	887(72)	375(36)	302(49)	0	0	-53(31)
N ⁽³⁾	0.0	0.8812 (9)	0.6367 (10)	1030(58)	263(27)	331(35)	0	0	-25(27)
N ⁽⁴⁾	0.0	0.6160 (9)	0.8282 (9)	1159(70)	274(29)	335(36)	0	0	-64(27)
C ⁽¹⁾	0.1262 (10)	0.7055 (13)	0.1635 (15)	335(38)	804(55)	657(75)	-25(32)	-27(48)	155(43)
C ⁽²⁾	0.1245 (11)	0.7767 (11)	0.3057 (14)	494(51)	827(59)	554(69)	108(38)	284(53)	180(38)
C ⁽³⁾	0.1273 (9)	0.8367 (12)	0.7127 (10)	427(32)	683(41)	544(47)	-184(34)	-93(34)	243(38)
C ⁽⁴⁾	0.1245 (10)	0.6527 (13)	0.7486 (9)	614(39)	630(51)	537(49)	294(42)	210(39)	203(38)
H ^{(N(1), 1)}	0.0	0.8680(125)	0.0508 (89)	600					
H ^{(N(1), 2)}	0.0	0.7026(126)	0.0035(121)	600					
H ^{(N(2))}	0.0	0.6295(144)	0.3730(132)	600					
H ^{(N(3), 1)}	0.0	0.9817(133)	0.6180(122)	600					
H ^{(N(3), 2)}	0.0	0.7908(139)	0.5631(124)	600					
H ^{(N(4))}	0.0	0.5104(134)	0.8508(114)	600					
H ^{(C(1), 1)}	0.1238 (82)	0.5948(101)	0.1551 (77)	600					
H ^{(C(1), 2)}	0.1977(116)	0.7486 (81)	0.1279(129)	600					
H ^{(C(2), 1)}	0.2016(102)	0.7411 (82)	0.3593(108)	600					
H ^{(C(2), 2)}	0.1146 (90)	0.9013 (98)	0.2946 (88)	600					
H ^{(C(3), 1)}	0.2063 (71)	0.8653 (94)	0.6736 (69)	600					
H ^{(C(3), 2)}	0.1319 (78)	0.9059 (89)	0.8013 (81)	600					
H ^{(C(4), 1)}	0.1332 (74)	0.5657 (97)	0.6711 (76)	600					
H ^{(C(4), 2)}	0.2075 (67)	0.6289 (83)	0.8153 (67)	600					

tion is centrosymmetric. Figure 1 shows a sketch of this cation. The intramolecular distances for the H_2O and some interionic distances for piperazinium dibromide monohydrate are given in Table 6. Figure 2 shows the overall structure of the piperazinium monocation, $[\text{C}_4\text{H}_{11}\text{N}_2]^+$. There are two mono-cations in the asymmetric unit of the elementary cell. Intramolecular distances and angles for the piperazinium monocations 1 and 2, appearing in the lattice of piper-

azinium monoiodide, are listed in Table 7. Interionic distances for piperazinium monoiodide are given in Table 8.

^{79}Br and ^{127}I NQR

In Fig. 3 the ^{79}Br NQR frequencies of 1,2-diammoniumethane dibromide, $\text{C}_2\text{H}_{10}\text{Br}_2\text{N}_2$, and of 1,3-diammoniumpropane dibromide, $\text{C}_3\text{H}_{12}\text{Br}_2\text{N}_2$, are plotted as a function of temperature. The curves

Table 5. Intramolecular distances (in pm) and angles (in degree) in the piperazinium di-cation $[\text{C}_4\text{H}_{12}\text{N}_2]^{2+}$ in piperazinium dibromide monohydrate. Errors are given in brackets. See Fig. 1.

$A-B$	d	$(A-B-C)$	\angle
$\text{C}^{(1)}-\text{H}^{(\text{C}(1),1)}$	108.5 (40)	$\text{N}-\text{C}^{(1)}-\text{C}^{(2)}$	110.9 (2)
$\text{C}^{(1)}-\text{H}^{(\text{C}(1),2)}$	104.3 (44)	$\text{H}^{(\text{C}(1),1)}-\text{C}^{(1)}-\text{N}$	107.3 (29)
$\text{C}^{(1)}-\text{C}^{(2)}$	151.4 (4)	$\text{H}^{(\text{C}(1),1)}-\text{C}^{(1)}-\text{C}^{(2)}$	109.3 (27)
$\text{C}^{(2)}-\text{H}^{(\text{C}(2),1)}$	97.5 (48)	$\text{H}^{(\text{C}(1),1)}-\text{C}^{(1)}-\text{H}^{(\text{C}(1),2)}$	121.5 (33)
$\text{C}^{(2)}-\text{H}^{(\text{C}(2),2)}$	98.9 (45)	$\text{H}^{(\text{C}(1),2)}-\text{C}^{(1)}-\text{N}$	106.5 (23)
$\text{C}^{(2)}-\text{N}$	149.8 (3)	$\text{H}^{(\text{C}(1),2)}-\text{C}^{(1)}-\text{C}^{(2)}$	101.2 (25)
$\text{N}-\text{H}^{(\text{N},1)}$	95.8 (49)	$\text{C}^{(1)}-\text{C}^{(2)}-\text{N}$	109.9 (2)
$\text{N}-\text{H}^{(\text{N},2)}$	83.8 (48)	$\text{H}^{(\text{C}(2),1)}-\text{C}^{(2)}-\text{N}$	103.9 (29)
$\text{N}-\text{C}^{(1)}$	148.4 (3)	$\text{H}^{(\text{C}(2),1)}-\text{C}^{(2)}-\text{C}^{(1)}$	113.7 (29)
		$\text{H}^{(\text{C}(2),1)}-\text{C}^{(2)}-\text{H}^{(\text{C}(2),2)}$	110.1 (36)
		$\text{H}^{(\text{C}(2),2)}-\text{C}^{(2)}-\text{N}$	101.7 (27)
		$\text{H}^{(\text{C}(2),2)}-\text{C}^{(2)}-\text{C}^{(1)}$	116.1 (26)
		$\text{C}^{(2)}-\text{N}-\text{C}^{(1)}$	110.8 (2)
		$\text{H}^{(\text{N},1)}-\text{N}-\text{C}^{(1)}$	113.0 (27)
		$\text{H}^{(\text{N},1)}-\text{N}-\text{C}^{(2)}$	105.3 (24)
		$\text{H}^{(\text{N},1)}-\text{N}-\text{H}^{(\text{N},2)}$	108.3 (39)
		$\text{H}^{(\text{N},2)}-\text{N}-\text{C}^{(1)}$	110.6 (30)
		$\text{H}^{(\text{N},2)}-\text{N}-\text{C}^{(2)}$	109.4 (33)

Table 6. Intramolecular distance and angle for H_2O and interionic distances (in pm) and angles (in degree) for piperazinium dibromide monohydrate $\text{C}_4\text{H}_{14}\text{Br}_2\text{N}_2\text{O}$. Errors are given in brackets. See Fig. 1.

Distances	d	Angles	\angle
$\text{O}-\text{H}$	84.7 (45)	$\text{H}^{(\text{O})}-\text{O}-\text{H}^{(\text{O})}$	111.0 (60)
$\text{N} \dots \text{Br}$	329.6	$\text{N}-\text{H}^{(\text{N},1)} \dots \text{Br}$	135.6
	335.9		114.7
	344.6	$\text{N}-\text{H}^{(\text{N},2)} \dots \text{Br}$	164.8
$\text{H}^{(\text{N},1)} \dots \text{Br}$	260.8		
	293.6	$\text{O}-\text{H}^{(\text{O})} \dots \text{Br}$	155.7
$\text{H}^{(\text{N},2)} \dots \text{Br}$	248.0	$\text{N}-\text{H}^{(\text{N},1)} \dots \text{O}$	112.4
	329.2		
$\text{Br} \dots \text{O}$	348.1		
$\text{H}^{(\text{O})} \dots \text{Br}$	269.4		
$\text{N} \dots \text{O}$	306.1		
$\text{H}^{(\text{N},1)} \dots \text{O}$	256.6		
$\text{H}^{(\text{N},2)} \dots \text{O}$	294.9		

Table 7. Intramolecular distances (in pm) and angles (in degree) in the two piperazinium mono-cations $[\text{C}_4\text{H}_{11}\text{N}_2]^+$ in piperazinium monoiodide. Errors are given in brackets. See Fig. 2.

$A-B$	d	$(A-B-C)$	\angle	$(A-B-C)$	\angle
$\text{N}^{(1)}-\text{H}^{(\text{N}(1),1)}$	91.6 (93)	$\text{C}^{(1)}-\text{N}^{(1)}-\text{C}^{(1)}$	109.6 (11)	$\text{H}^{(\text{N}(3),2)}-\text{N}^{(3)}-\text{C}^{(3)}$	101.8 (33)
$\text{N}^{(1)}-\text{H}^{(\text{N}(1),2)}$	95.7 (107)	$\text{H}^{(\text{N}(1),1)}-\text{N}^{(1)}-\text{C}^{(1)}$	117.9 (22)	$\text{N}^{(\text{N}(3),1)}-\text{N}^{(3)}-\text{H}^{(\text{N}(3),2)}$	120.6 (106)
$\text{N}^{(1)}-\text{C}^{(1)}$	148.0 (12)	$\text{H}^{(\text{N}(1),2)}-\text{N}^{(1)}-\text{C}^{(1)}$	107.7 (35)	$\text{N}^{(3)}-\text{C}^{(3)}-\text{C}^{(4)}$	109.6 (7)
$\text{C}^{(1)}-\text{H}^{(\text{C}(1),1)}$	86.5 (75)	$\text{H}^{(\text{N}(1),1)}-\text{N}^{(1)}-\text{H}^{(\text{N}(1),2)}$	93.8 (87)	$\text{H}^{(\text{C}(3),1)}-\text{C}^{(3)}-\text{N}^{(3)}$	115.4 (45)
$\text{C}^{(1)}-\text{H}^{(\text{C}(1),2)}$	83.9 (106)	$\text{N}^{(1)}-\text{C}^{(1)}-\text{C}^{(2)}$	110.5 (10)	$\text{H}^{(\text{C}(3),1)}-\text{C}^{(3)}-\text{C}^{(4)}$	111.5 (51)
$\text{C}^{(1)}-\text{C}^{(2)}$	151.1 (9)	$\text{H}^{(\text{C}(1),1)}-\text{C}^{(1)}-\text{N}^{(1)}$	102.5 (53)	$\text{H}^{(\text{C}(3),1)}-\text{C}^{(3)}-\text{H}^{(\text{C}(3),2)}$	101.9 (56)
$\text{C}^{(2)}-\text{H}^{(\text{C}(2),1)}$	95.1 (100)	$\text{H}^{(\text{C}(1),1)}-\text{C}^{(1)}-\text{C}^{(2)}$	117.0 (56)	$\text{H}^{(\text{C}(3),2)}-\text{C}^{(3)}-\text{N}^{(3)}$	110.3 (42)
$\text{C}^{(2)}-\text{H}^{(\text{C}(2),2)}$	97.9 (78)	$\text{H}^{(\text{C}(1),1)}-\text{C}^{(1)}-\text{H}^{(\text{C}(1),2)}$	112.2 (70)	$\text{H}^{(\text{C}(3),2)}-\text{C}^{(3)}-\text{C}^{(4)}$	107.6 (37)
$\text{C}^{(2)}-\text{N}^{(2)}$	144.5 (14)	$\text{H}^{(\text{C}(1),2)}-\text{C}^{(1)}-\text{N}^{(1)}$	110.0 (78)	$\text{C}^{(3)}-\text{C}^{(4)}-\text{N}^{(4)}$	109.5 (8)
$\text{N}^{(2)}-\text{H}^{(\text{N}(2))}$	76.0 (111)	$\text{H}^{(\text{C}(1),2)}-\text{C}^{(1)}-\text{C}^{(2)}$	104.7 (81)	$\text{H}^{(\text{C}(4),1)}-\text{C}^{(4)}-\text{N}^{(4)}$	109.9 (41)
$\text{N}^{(3)}-\text{H}^{(\text{N}(3),1)}$	80.3 (99)	$\text{C}^{(1)}-\text{C}^{(2)}-\text{N}^{(2)}$	112.0 (10)	$\text{H}^{(\text{C}(4),1)}-\text{C}^{(4)}-\text{C}^{(3)}$	117.2 (46)
$\text{N}^{(3)}-\text{H}^{(\text{N}(3),2)}$	101.2 (120)	$\text{H}^{(\text{C}(2),1)}-\text{C}^{(2)}-\text{N}^{(2)}$	106.6 (60)	$\text{H}^{(\text{C}(4),1)}-\text{C}^{(4)}-\text{H}^{(\text{C}(4),2)}$	107.1 (49)
$\text{N}^{(3)}-\text{C}^{(3)}$	147.4 (11)	$\text{H}^{(\text{C}(2),1)}-\text{C}^{(2)}-\text{C}^{(1)}$	113.8 (58)	$\text{H}^{(\text{C}(4),2)}-\text{C}^{(4)}-\text{N}^{(4)}$	104.3 (38)
$\text{C}^{(3)}-\text{H}^{(\text{C}(3),1)}$	87.9 (66)	$\text{H}^{(\text{C}(2),1)}-\text{C}^{(2)}-\text{H}^{(\text{C}(2),2)}$	115.2 (57)	$\text{H}^{(\text{C}(4),2)}-\text{C}^{(4)}-\text{C}^{(3)}$	108.0 (40)
$\text{C}^{(3)}-\text{H}^{(\text{C}(3),2)}$	103.0 (83)	$\text{H}^{(\text{C}(2),2)}-\text{C}^{(2)}-\text{N}^{(2)}$	103.9 (53)	$\text{C}^{(4)}-\text{N}^{(4)}-\text{C}^{(4)}$	109.9 (8)
$\text{C}^{(3)}-\text{C}^{(4)}$	147.3 (11)	$\text{H}^{(\text{C}(2),2)}-\text{C}^{(2)}-\text{C}^{(1)}$	105.0 (51)	$\text{H}^{(\text{N}(4))}-\text{N}^{(4)}-\text{C}^{(4)}$	109.3 (38)
$\text{C}^{(4)}-\text{H}^{(\text{C}(4),1)}$	102.6 (67)	$\text{C}^{(2)}-\text{N}^{(2)}-\text{C}^{(2)}$	111.2 (11)		
$\text{C}^{(4)}-\text{H}^{(\text{C}(4),2)}$	104.9 (64)	$\text{H}^{(\text{N}(2))}-\text{N}^{(2)}-\text{C}^{(2)}$	103.4 (53)		
$\text{C}^{(4)}-\text{N}^{(4)}$	145.8 (12)	$\text{C}^{(3)}-\text{N}^{(3)}-\text{C}^{(3)}$	111.7 (9)		
$\text{N}^{(4)}-\text{H}^{(\text{N}(4))}$	85.0 (106)	$\text{H}^{(\text{N}(3),1)}-\text{N}^{(3)}-\text{C}^{(3)}$	110.2 (41)		

are smooth and no sign of a phase transition is observed. In contrast to 1,2-diammoniummethane dibromide, 1,2-diammoniummethane diiodide, $\text{C}_2\text{H}_{10}\text{I}_2\text{N}_2$, shows phase transitions. In Fig. 4 the ^{127}I NQR frequencies are plotted as a function of temperature for this compound. Jumps are observed in $\nu(T)$ for both transitions, $\nu_1(m = \pm 1/2 \leftrightarrow m = \pm 3/2)$ and $\nu_2(m = \pm 3/2 \leftrightarrow m = \pm 5/2)$. As can be seen, the transitions are more strongly revealed by the transition $m = 1/2 \leftrightarrow$

$m = 3/2$ than by $m = 3/2 \leftrightarrow m = 5/2$. By solving the secular equation [9], from the ^{127}I NQR transitions the nuclear quadrupole coupling constant (NQCC), $eQ\Phi_{zz}h^{-1}$ (^{127}I), follows. e is the unit charge, Q the nuclear quadrupole moment, h Planck's constant and $\Phi_{zz} = e q$ the z -axis of the electric field gradient tensor with its principal axes Φ_{xx} , Φ_{yy} , and Φ_{zz} ($\Phi_{zz} \geq \Phi_{yy} \geq \Phi_{xx}$). In Fig. 5 the asymmetry parameter η (^{127}I) of 1,2-diammoniummethane diiodide is shown as a func-

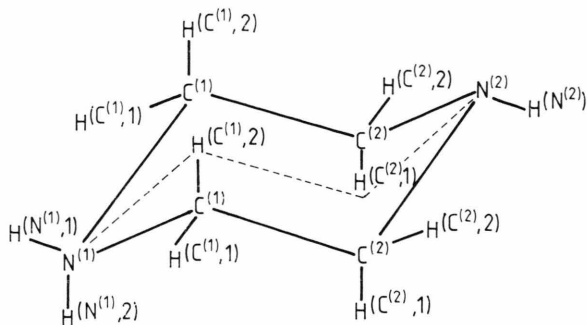


Fig. 2. Sketch of the piperazinium mono-cation $[\text{C}_4\text{H}_{11}\text{N}_2]^+$ in the lattice of piperazinium monoiodide. Only one of the two crystallographically independent cations within the asymmetric unit of the unit cell is shown. For the second cation: $\text{C}^{(1)} \rightarrow \text{C}^{(3)}$, $\text{C}^{(2)} \rightarrow \text{C}^{(4)}$, $\text{N}^{(1)} \rightarrow \text{N}^{(3)}$, $\text{N}^{(2)} \rightarrow \text{N}^{(4)}$, and so on.

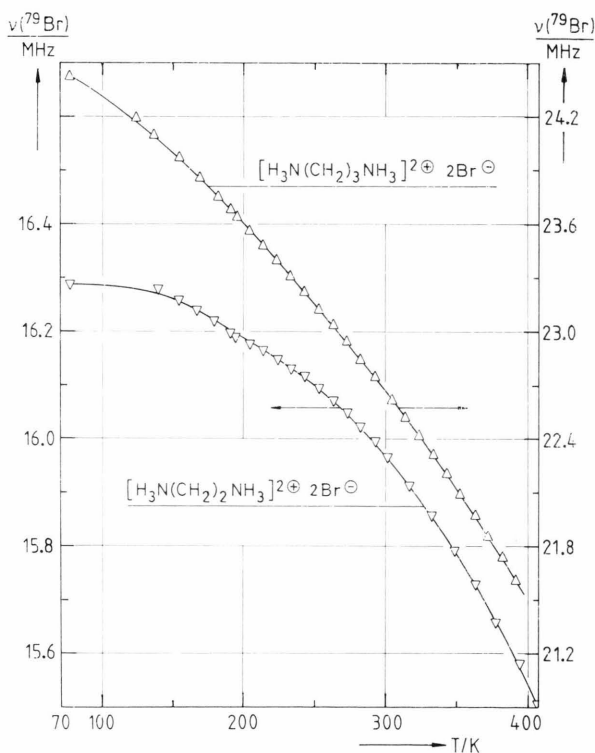


Fig. 3. ^{79}Br NQR frequencies of 1,2-diammoniummethane dibromide and 1,3-diammoniumpropane dibromide as a function of temperature.

tion of temperature as is $eQ\Phi_{zz}h^{-1}(^{127}\text{I})$. Both, the NQCC and η show the two phase transitions, one at about 400 K, one at about 404 K, and it is interesting to note that in two of the phases, in the low temperature phase III of $\text{C}_2\text{H}_{10}\text{I}_2\text{N}_2$ and in the middle phase

Table 8. Intermolecular distances (in pm) and angles (in degree) in piperazinium monoiodide $\text{C}_4\text{H}_{11}\text{IN}_2$.

Distances	<i>d</i>	Angles	\angle
$\text{N}^{(1)} \dots \text{I}^{(1)}$	353.6	$\text{N}^{(1)}-\text{H}^{(\text{N}(1),1)} \dots \text{I}^{(1)}$	166.6
$\text{N}^{(2)} \dots \text{I}^{(1)}$	497.0	$\text{N}^{(4)}-\text{H}^{(\text{N}(4))} \dots \text{I}^{(1)}$	163.7
$\text{N}^{(3)} \dots \text{I}^{(1)}$	437.1	$\text{N}^{(3)}-\text{H}^{(\text{N}(3),1)} \dots \text{I}^{(2)}$	159.2
$\text{N}^{(4)} \dots \text{I}^{(1)}$	364.2	$\text{N}^{(2)}-\text{H}^{(\text{N}(2))} \dots \text{I}^{(2)}$	158.2
$\text{N}^{(1)} \dots \text{I}^{(2)}$	495.2		
$\text{N}^{(2)} \dots \text{I}^{(2)}$	364.9		
$\text{N}^{(3)} \dots \text{I}^{(2)}$	347.1		
$\text{N}^{(4)} \dots \text{I}^{(2)}$	505.5		
$\text{H}^{(\text{N}(1),1)} \dots \text{I}^{(1)}$	263.8		
$\text{H}^{(\text{N}(1),2)} \dots \text{I}^{(1)}$	387.5		
$\text{H}^{(\text{N}(4))} \dots \text{I}^{(1)}$	281.9		
$\text{H}^{(\text{N}(2))} \dots \text{I}^{(2)}$	293.3		
$\text{H}^{(\text{N}(3),1)} \dots \text{I}^{(2)}$	270.8		
$\text{H}^{(\text{N}(3),2)} \dots \text{I}^{(2)}$	385.2		

II, the asymmetry parameter $\eta(^{127}\text{I})$ is non-zero, whereas it is zero for the high temperature phase I.

For 1,3-diammoniumpropane diiodide, $\text{C}_3\text{H}_{12}\text{I}_2\text{N}_2$, we have observed a phase transition, too. In Fig. 6 the ^{127}I NQR frequencies are plotted as a function of temperature and Fig. 7 shows the NQCC for the two crystallographically inequivalent iodine ions together with the corresponding asymmetry parameters.

The ^{79}Br NQR of piperazinium dibromide monohydrate, $\text{C}_4\text{H}_{14}\text{Br}_2\text{N}_2\text{O}$, is a smooth one line spectrum in the whole temperature range we have followed up. The curve $\nu(^{79}\text{Br}) = f(T)$ is given in Figure 8. Finally we have studied piperazinium monoiodide, $\text{C}_4\text{H}_{11}\text{IN}_2$. In Fig. 9 the ^{127}I NQR frequencies are shown as a function of temperature. There are two iodine ions in the asymmetric unit cell of this compound, and accordingly four ^{127}I NQR lines are observed. Single crystal work or a spin echo double resonance, SEDOR, experiment would be necessary to assign the two transitions $m = \pm 1/2 \leftrightarrow m = \pm 3/2$ and the two transitions $m = \pm 3/2 \leftrightarrow m = \pm 5/2$ to the two crystallographically independent iodine atoms. Due to the lack of information, we are unable to extract from the resonance frequencies the NQCC's and the η 's. However, from the resonance frequencies we find a phase transition at $T \approx 196$ K which is most probably of higher order than 1.

The experimental results $\nu(^{79}\text{Br}, ^{127}\text{I})$ can be rationalized by a polynomial

$$\nu_i(T) = \sum_i (a_i T^i), \quad i = -1, \dots, 2. \quad (1)$$

In Table 9 the parameters a_i are listed for the compounds studied and for the temperature range covered.

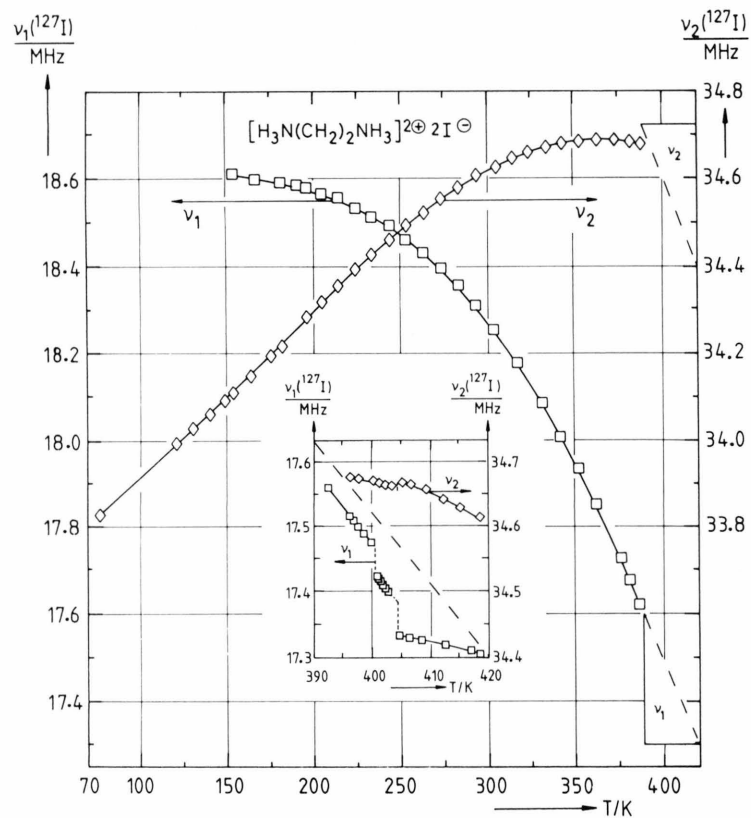


Fig. 4. ^{127}I NQR frequencies of 1,2-diammoniummethane diiodide, $\text{C}_2\text{H}_{10}\text{I}_2\text{N}_2$, as a function of temperature. The region of phase transition is drawn in enlarged scale in the insert.

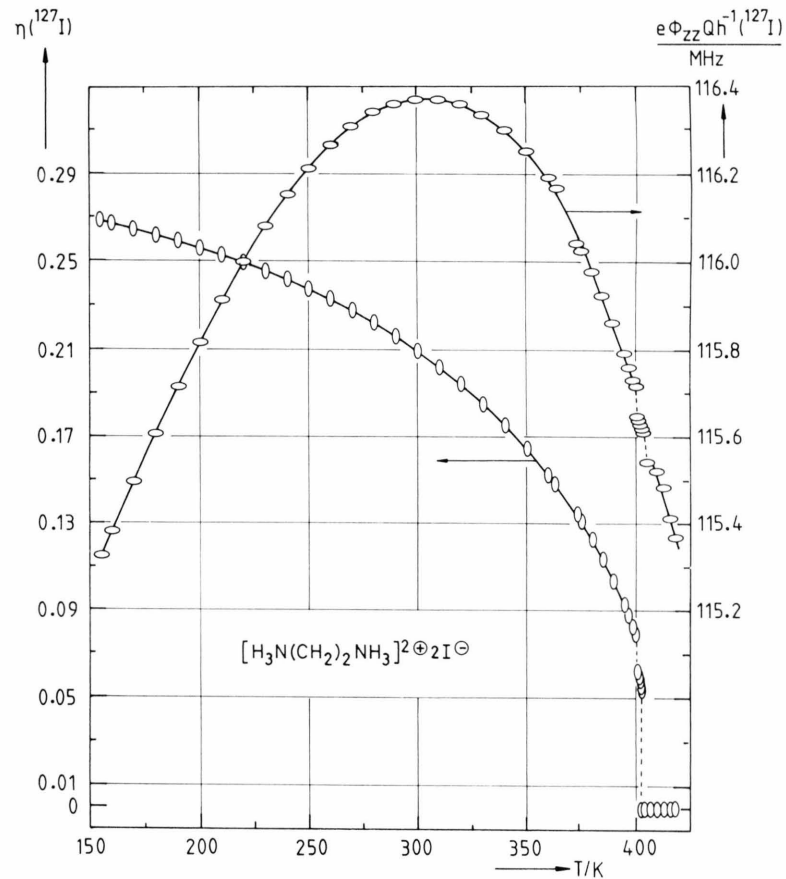


Fig. 5. Nuclear quadrupole coupling constant $eQ\Phi_{zz}h^{-1}(^{127}\text{I})$ and asymmetry parameter $\eta(^{127}\text{I})$ of 1,2-diammoniummethane diiodide as a function of temperature.

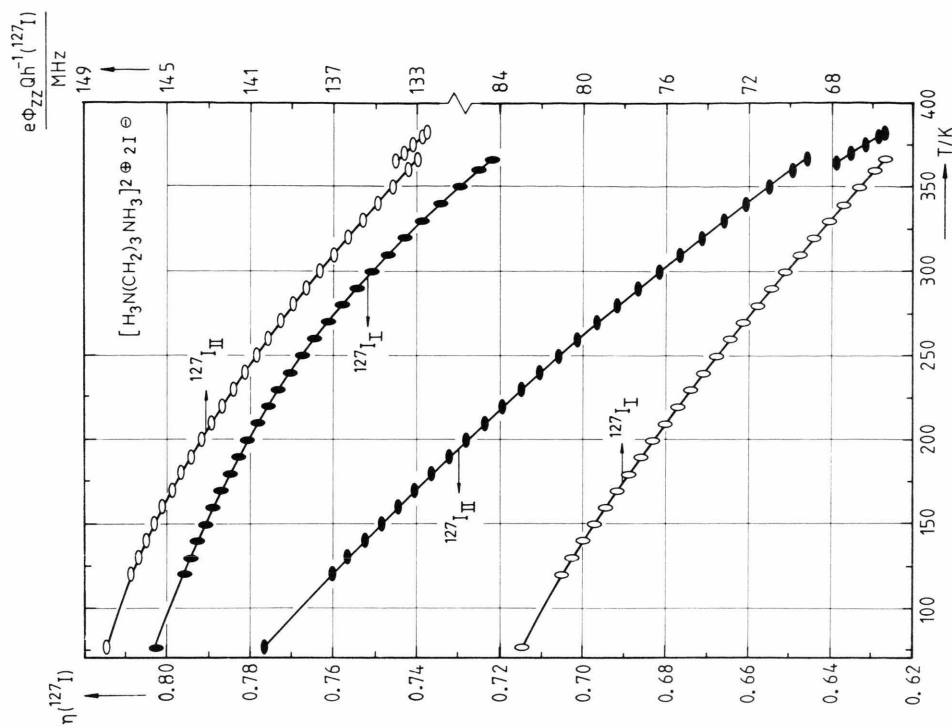


Fig. 7. Nuclear quadrupole coupling constants $eQ_{zz}Qh^{-1}(^{127}\text{I})$ and asymmetry parameters $\eta(^{127}\text{I})$ of 1,3-diammoniumpropane diiodide as a function of temperature.

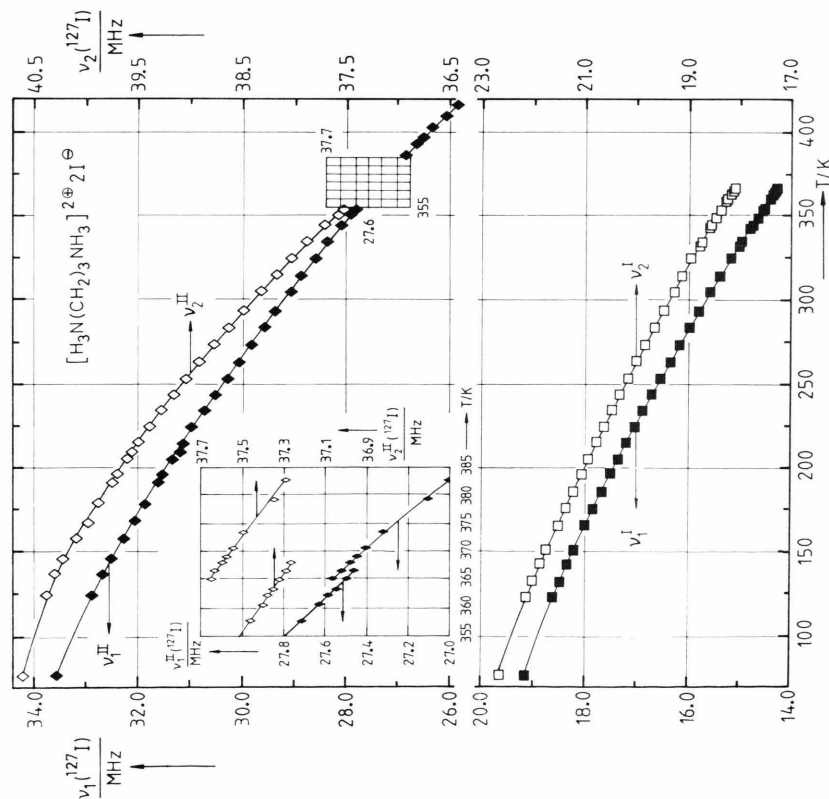


Fig. 6. ^{127}I NQR frequencies of 1,3-diammoniumpropane diiodide as a function of temperature. The region of phase transition is drawn in enlarged scale in the insert.

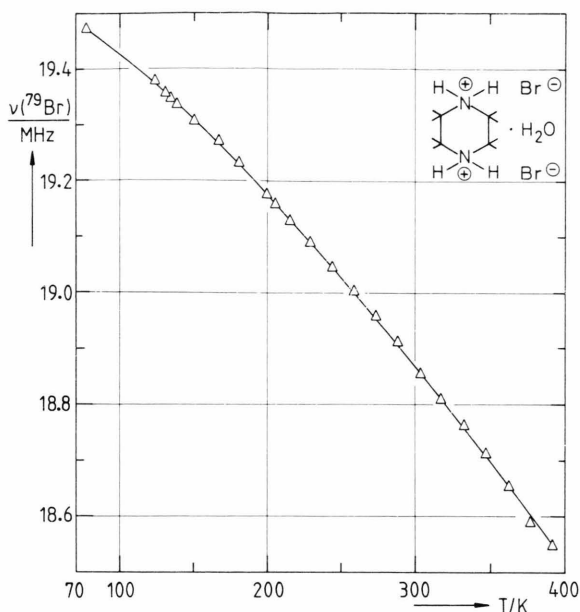


Fig. 8. $\nu(^{79}\text{Br})$ of piperazinium dibromide monohydrate as a function of temperature.

In case of a phase transition the temperature range is broken up in appropriate sections. Finally, in Table 10, we give, for convenience, $\nu(^{79}\text{Br})$ and $\nu(^{127}\text{I})$ of the title compounds for a few selected temperatures.

Discussion

Piperazinium Dibromide Monohydrate

In the solid state of piperazinium dibromide monohydrate, $\text{C}_4\text{H}_{12}\text{Br}_2\text{N}_2 \cdot \text{H}_2\text{O}$, we find a monoclinic lattice, space group $\text{C}_{2h}^6 - \text{C}2/c$ with $Z = 4$ formula units in the unit cell, built up from piperazinium di-cations, $[\text{C}_4\text{H}_{12}\text{N}_2]^{2+}$, bromide ions, Br^- , and molecules H_2O . The di-cation has chair conformation (see Fig. 1) with a center of symmetry at the center of the plane of the four carbon atoms. The molecules H_2O are located at an axis 2. The nitrogen atoms as well as the carbon atoms are nearly tetrahedrally coordinated and the deviations of the angles $\text{C}^{(1)} - \text{N} - \text{C}^{(2)}$, $\text{N} - \text{C}^{(2)} - \text{C}^{(1)}$, and $\text{N} - \text{C}^{(1)} - \text{C}^{(2)}$ from 109° are quite small ($\leq 1.9^\circ$). The distances $\text{C} - \text{N}$ are 148.4 pm

Table 9. Power series expansion for the NQR frequencies $\nu = f(T)$ of the investigated compounds. $f(T)$ is of the form $f(T) = \sum_i a_i \cdot T^i$. ΔT = temperature range, z = number of experimental points, σ = standard deviation.

Compound	Nucl.	Assign (see Figs. 3–9)	$\Delta T/\text{K}$	z	σ/kHz	$\frac{a_{-1}}{\text{MHz} \cdot \text{K}}$	$\frac{a_0}{\text{MHz}}$	$\frac{10^3 \cdot a_1}{\text{MHz} \cdot \text{K}^{-1}}$	$\frac{10^6 \cdot a_2}{\text{MHz} \cdot \text{K}^{-2}}$
1,2-Diammonium-ethane dibromide	^{79}Br		77 –405.6	25	9.3	14.672	15.934	2.945	– 9.99
1,2-Diammonium-ethane diiodide	^{127}I	ν_2	77 –363.1	27	9.0	38.475	32.664	9.601	–11.81
	^{127}I	ν_2	373.5–403.5	9	2.0	–480.697	31.682	25.795	–38.31
	^{127}I	ν_2	405.3–418.2	6	6.6	–17775.500	108.457	–39.633	–84.44
	^{127}I	ν_1	154.2–400.0	30	2.4	151.320	16.030	15.171	–31.25
	^{127}I	ν_1	400.8–403.0	6	2.0	1638.380	13.334	0.000	0.00
	^{127}I	ν_1	404.7–418.5	6	4.7	–8331.153	45.573	12.141	–76.75
1,3-Diammonium-propane dibromide	^{79}Br		77 –392.0	28	8.1	–10.196	24.989	– 4.657	– 9.85
1,3-Diammonium-propane diiodide	^{127}I	ν_2^{II}	77 –367.9	35	15.3	–21.919	41.287	– 3.700	–19.08
	^{127}I	ν_2^{II}	364.9–382.8	8	12.6	–9322.787	93.580	–79.193	–11.10
	^{127}I	ν_1^{II}	77 –366.4	34	21.1	–13.659	34.866	–12.794	–19.79
	^{127}I	ν_1^{II}	364.9–416.9	14	14.1	6676.109	–17.128	125.884	–146.67
	^{127}I	ν_2^{I}	77 –366.4	35	18.7	–14.679	23.756	–10.947	–11.83
	^{127}I	ν_1^{I}	77 –366.4	35	12.6	–9.095	20.159	–10.109	–16.01
Piperazinium dibromide monohydrate	^{79}Br		77 –392.2	23	4.0	–2.536	19.665	– 1.880	– 2.47
Piperazinium monoiodide	^{127}I	ν_4	77 –192.7	16	6.7	90.287	35.206	21.251	–23.45
	^{127}I	ν_4	194.8–342.6	14	4.4	–622.854	46.082	–23.489	15.75
	^{127}I	ν_3	77 –194.7	16	16.8	–225.403	34.597	–57.949	246.22
	^{127}I	ν_3	196.6–316.3	10	5.3	–172.472	32.462	2.439	–12.75
	^{127}I	ν_2	77 –196.0	17	10.3	– 86.912	26.378	–19.719	82.86
	^{127}I	ν_2	197.2–356.1	22	4.0	–209.563	27.155	– 4.317	1.11
	^{127}I	ν_1	77 –196.0	17	19.6	–216.769	28.514	–51.881	186.66
	^{127}I	ν_1	197.2–356.1	21	5.7	55.611	23.754	4.677	–11.92

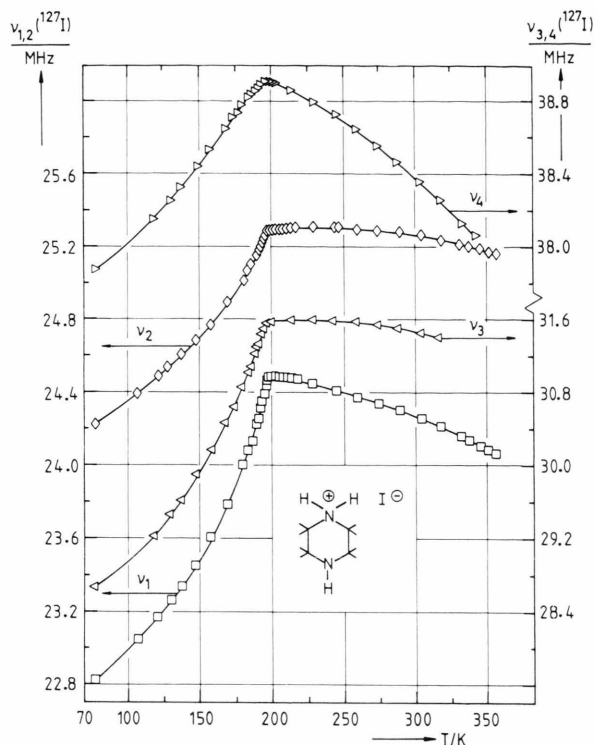


Fig. 9. ^{127}I NQR frequencies as a function of temperature for piperazinium monoiodide.

and 149.8 pm, slightly larger than $d(\text{C}-\text{N})$ found in anilinium salts (144.5–147.6 pm) [4]. The carbon–carbon distance is within the range expected. We can compare the compound with piperazinium dichloride monohydrate, which is isotypic to piperazinium dibromide monohydrate. Rérat [10] reports (our data for the bromide in brackets $a = 1021$ pm (1148.7 pm), $b = 634$ pm (590.5 pm), $c = 1350$ pm (1501.6 pm), and $\beta = 107.5^\circ$ (118.2°) in setting $\text{C}2/c$, $Z = 4$. For the distances $\text{C}-\text{N}$ he finds 149.0 pm (148.4 pm) and 150.9 pm (149.8 pm) and for the angles $\text{C}-\text{N}-\text{C}$ and $\text{N}-\text{C}-\text{C}$ he reports values between 109.3° (110.9°) and 113° (109.9°).

In Fig. 10a we show the crystal structure of piperazinium dibromide monohydrate, projected along the crystallographic axis $[b]$. The piperazinium di-cations are located with their centers of symmetry on planes parallel (bc) at $x = 0$ and $x = 1/2$; the molecules H_2O are centered at these layers, too. Parallel to the layers formed by $[\text{C}_4\text{H}_{12}\text{N}_2]^{2+}$ and H_2O , the bromide ions form undulated layers at $x = 1/4$ and $x = 3/4$, respectively. On the other hand, such a layered structure is also found parallel (ab) with $z = 0$ and $z = 1/2$ (cations), $\langle z \rangle = 1/4$ and $3/4$ (Br^- and H_2O). In total, no preferential packing is observed. A network of hydro-

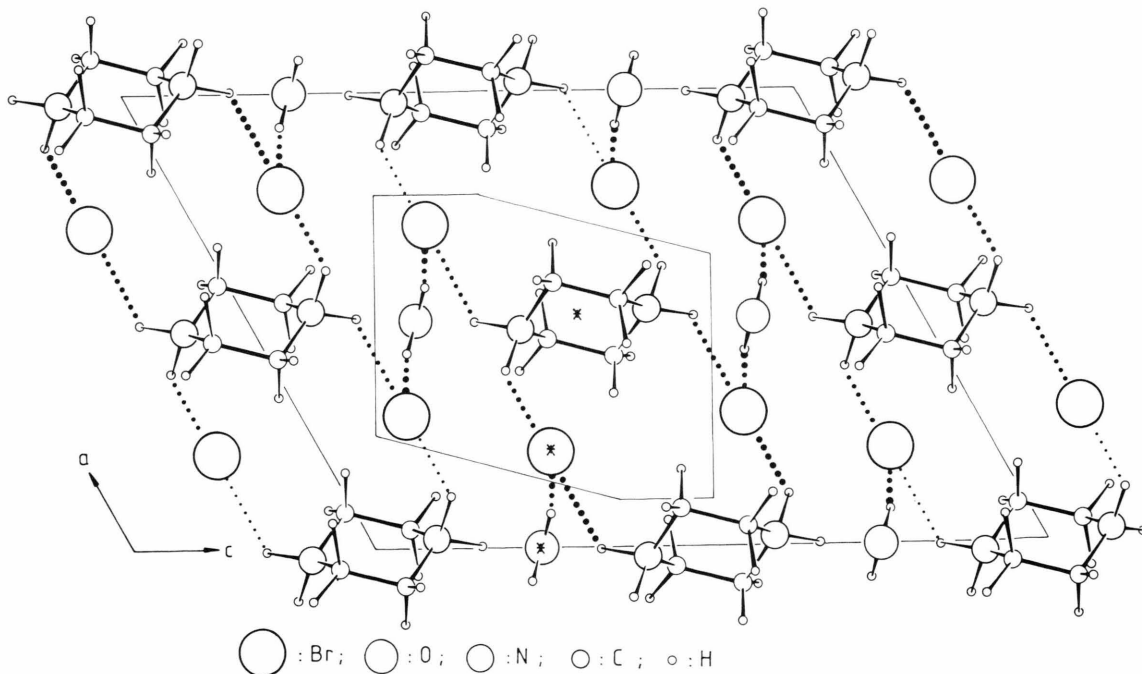
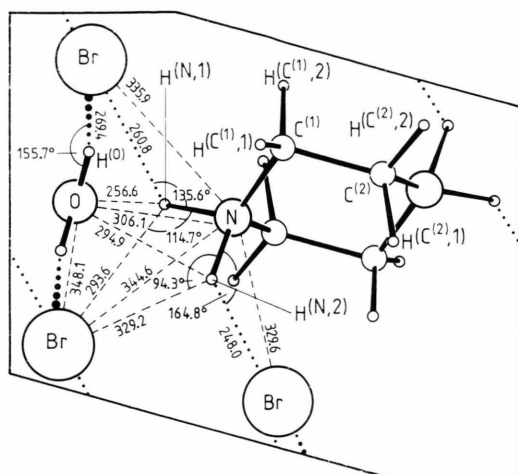
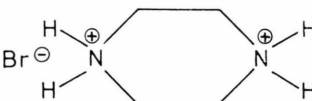



Fig. 10a. Projection of the crystal structure of piperazinium dibromide monohydrate along b onto the (ac) -plane. The positional parameters in Table 3 are given for the molecules and atoms marked by an asterisk. The dotted lines symbolize hydrogen bonds. Dots of different gauge mean that the hydrogen bonds are in different altitudes of the unit cell.



gen bonds connects the different layers; they are indicated in Fig. 10a (see also legend to this figure). Hydrogen bonds of the type $\text{N}-\text{H}^{(N)}\dots\text{Br}$ connect piperazinium di-cations via bromine anions in such a manner that they form ribbons at $z=0$ and $z=1/2$. These ribbons have different directions in space. The axes of the ribbons are $[110]$ at $z=0$ and $[\bar{1}10]$ at $z=1/2$, respectively. Two neighbouring ribbons (in direction c) are linked via water molecules which form hydrogen bonds of the type $\text{O}-\text{H}\dots\text{Br}$. These hydrogen bonds are probably weaker than the $\text{N}-\text{H}\dots\text{Br}$ bridges within one ribbon because the $\text{O}\dots\text{Br}$ distance is larger than the $\text{N}\dots\text{Br}$ distances, and the van der Waals radii of nitrogen and oxygen are similar (N: 150 pm, O: 140 pm) [11]. In Table 11 a scheme of the hydrogen bonds of piperazinium dibromide monohydrate and piperazinium monoiodide is given. Figure 10b gives the most prominent hydrogen bond distances and angles (detail of Figure 10). The bromine

Compound	<i>T</i> /K	$\nu(^{79}\text{Br})$ MHz	$\nu_2(^{127}\text{I})$ MHz	$\nu_1(^{127}\text{I})$ MHz	$\eta(^{127}\text{I})$	$e\Phi_{zz}Qh^{-1}(^{127}\text{I})$ MHz
$[\text{H}_3\text{N}(\text{CH}_2)_2\text{NH}_3]^{2+} \cdot 2\text{X}^-$	77	16.287	33.824			
	273.4	16.056	34.552	18.395	0.2258	116.335
	303.7	15.967	34.626	18.252	0.2063	116.396
$[\text{H}_3\text{N}(\text{CH}_2)_3\text{NH}_3]^{2+} \cdot 2\text{X}^-$	77	24.432	40.595	33.569	0.7761	147.911
			22.635	19.158	0.8026	82.843
	273.1	22.946	38.783	29.858	0.6953	139.395
			19.837	16.174	0.7601	72.083
	304.9	22.621	38.331	29.101	0.6796	137.408
			19.294	15.579	0.7491	69.979
 $\text{Br}^\ominus \cdot \text{H}_2\text{O}$	77	19.472				
	273.1	18.960				
	304.0	18.854				
 I^\ominus	77		37.876 ^a			
			28.670			
			24.224			
			22.818			
	273.3		38.562			
			31.541			
			25.285			
			24.338			
	303.2		38.360			
			31.459			
			25.285			
			24.257			

^a For this compound we are not able to decide clearly which two NQR frequencies belong to the same iodine atom. Therefore it is not possible to calculate the asymmetry parameters and the quadrupole coupling constants.

Table 11. Hydrogen bond scheme: hydrogen bond distances (in pm) and angles (in degree) in a) piperazinium dibromide monohydrate $\text{C}_4\text{H}_{14}\text{Br}_2\text{N}_2\text{O}$ (referred to Fig. 10b) and b) piperazinium monoiodide $\text{C}_4\text{H}_{11}\text{IN}_2$.

Atom A (coord.)	– atom H (coord.)	... atom X (coord.)	A...X	H...X	$\angle \text{A}–\text{H} \dots \text{X}$
a) Piperazinium dibromide monohydrate					
N (0.4784, 0.5378, 0.3987)	– H ^(N, 1) (0.5036, 0.5087, 0.3474)	... Br (0.7092, 0.3336, 0.3429)	335.9	260.8	135.6
	– H ^(N, 2) (0.4071, 0.6101, 0.3725)	... Br (0.2092, 0.8336, 0.3429)	329.6	248.0	164.8
O (0.5, 0.8679, 0.25)	– H ^(O) (0.4311, 0.9492, 0.2270)	... Br (0.2908, 0.3336, 0.1571)	348.1	269.4	155.7
b) Piperazinium monoiodide					
N ⁽¹⁾ (0, 0.7605, 0.0889)	– H ^{(N(1), 1)} (0, 0.8680, 0.0508)	... I ⁽¹⁾ (0, 1.2013, 0.0)	353.6	263.8	166.6
N ⁽²⁾ (0, 0.7272, 0.3784)	– H ^{(N(2), 1)} (0, 0.6295, 0.3730)	... I ⁽²⁾ (0, 0.2705, 0.4647)	364.9	293.3	158.2
N ⁽³⁾ (0, 0.8812, 0.6367)	– H ^{(N(3), 1)} (0, 0.9817, 0.6180)	... I ⁽²⁾ (0, 1.2705, 0.4647)	347.1	270.8	159.2
N ⁽⁴⁾ (0, 0.6160, 0.8282)	– H ^{(N(4), 1)} (0, 0.5104, 0.8508)	... I ⁽¹⁾ (0, 0.2013, 1.0)	364.2	281.9	163.7

NQR shows the classical Bayer-type behaviour [12] in its temperature dependence, see Figure 8. The temperature coefficient $d\nu/dT(^{79}\text{Br})$ is, however, rather strong for an ionic lattice and both, the hydrogen bonds and the librational motions of the cations and the H_2O may be responsible for this.

Piperazinium Monoiodide

Piperazinium monoiodide crystallizes with a non-centrosymmetric space group, $\text{C}_{2v}^7 - \text{Pmn}2_1$, $Z = 4$ formula units in the cell. There are two crystallographically inequivalent mono-cations in the unit cell. In Fig. 2 one of these cations is drawn and intramolecular distances and angles are given for both cations in Table 6. Both cations have chair conformation and the geometry of both is determined by mirror planes at which the atoms $\text{N}^{(1)}$, $\text{N}^{(2)}$, and $\text{H}^{(\text{N}, 2)}$, respectively $\text{N}^{(3)}$, $\text{N}^{(4)}$, and $\text{H}^{(\text{N}, 4)}$, are located. As in the piperazinium di-cation $[\text{C}_4\text{H}_{12}\text{N}_2]^{2+}$, in the mono-cation $[\text{C}_4\text{H}_{11}\text{N}_2]^+$ the angles $(\text{C}–\text{C}–\text{N})$ and $(\text{C}–\text{N}–\text{C})$ deviate little from 109° ($109.5^\circ \leq \varphi \leq 112.0^\circ$). The piperazinium mono-cation can be divided perpendicular to the mirror plane of it in two parts. The part with the protonated nitrogen atom corresponds to a piperazinium di-cation half section. The $\text{N}–\text{C}$ distances $\text{N}^{(1)}–\text{C}^{(1)} = 148.0$ pm and $\text{N}^{(3)}–\text{C}^{(3)} = 147.4$ pm are in the same range as the distances in the piperazinium di-cations in piperazinium dibromide monohydrate ($d(\text{N}–\text{C}) = 149.8$ pm, 148.4 pm), piperazinium dichloride monohydrate ($d(\text{N}–\text{C}) = 149.0$ pm and 150.9 pm [10]), and piperazinium hexachlorostannate trihydrate ($d(\text{C}–\text{N}) = 149.7$ pm [13]). These distances are slightly larger than the ones between the carbon atom and the lone pair carrying nitrogen atoms ($d(\text{N}^{(2)}–\text{C}^{(2)}) = 144.5$ pm and $d(\text{N}^{(4)}–\text{C}^{(4)}) = 145.8$

pm) which are nearly the same as the $\text{C}–\text{N}$ distances in piperazine hexahydrate ($d(\text{C}–\text{N}) = 145.8$ pm and 145.9 pm [14]). In Fig. 11 the projection of the crystal structure of piperazinium monoiodide is shown along the axis [100]. In the chosen setting, $\text{Pmn}2_1$, the c -axis of the crystal is the polar one. The polarity is mainly – and visible – due to the polar orientation of the piperazinium mono-cations. The non-protonated nitrogens of the two crystallographically independent cations, $\text{N}^{(2)}$ and $\text{N}^{(4)}$ are located on the plus-side of the cation (if we introduce a direction in Fig. 11 going from $z = 0$ to $z = 1$). Piperazinium monoiodide crystallizes with a layer structure; the nitrogen atoms, the hydrogen atoms at the nitrogens, and the iodine ions are located at $x = 0$ and $x = 1/2$. The space between is filled by the CH_2 groups of the cations, and the C_4 plane of the piperazinium ring is perpendicular to the plane (bc) . The two independent piperazinium ions are practically perpendicular to each other (the C_4 planes form an angle of 82.4° (see Figure 11)). The hydrogen bonds $\text{N}–\text{H} \dots \text{I}$ connect anions and cations; thereby chains are formed nearly parallel to $[012]$ and $[0\bar{1}2]$. Hydrogen bond distances and angles for piperazinium dibromide and piperazinium monoiodide are listed in Table 11. There is no hydrogen bond contact and only weak van der Waals interaction between the two layers at $x = 0$ and $x = 1/2$.

In Table 12 interionic distances and angles of hydrogen bonds are listed for organic ammonium bromides and iodides; halogen NQR data are available for all compounds considered.

The ^{127}I NQR spectrum of piperazinium monoiodide reflects the results of the crystal structure determination. Two crystallographically independent iodines are found. Further experiments are necessary to determine the asymmetry parameters η and the

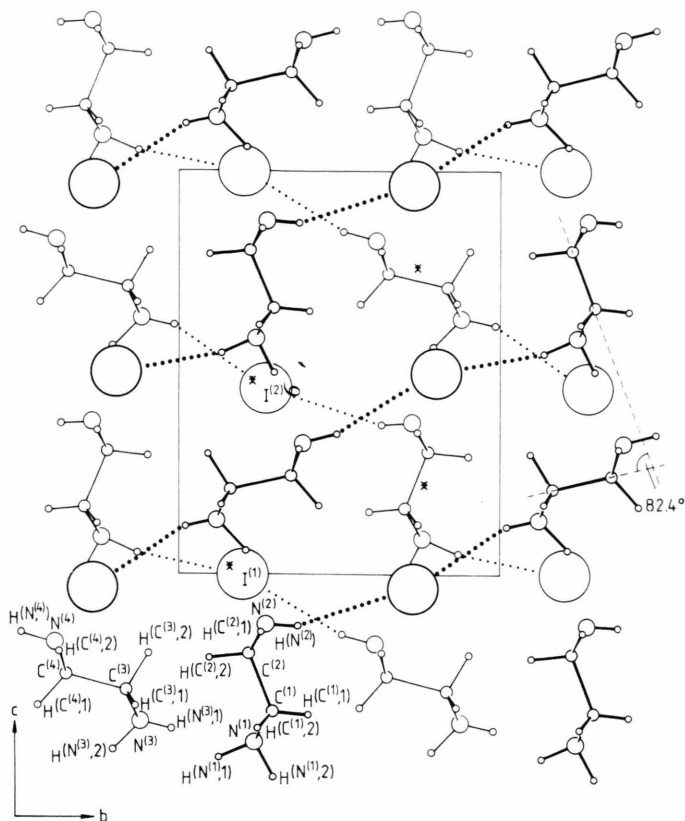


Fig. 11. Projection of the crystal structure of piperazinium monoiodide along a onto the $(b\ c)$ -plane. For the molecules and atoms marked by an asterisk the positional parameters are given in Table 4. The dotted lines symbolize hydrogen bonds. These hydrogen bonds are in the $(b\ c)$ -plane at $x = 0$ (.....) and $x = 1/2$ (●●●●), respectively.

nuclear quadrupole coupling constants e^2qQh^{-1} (^{127}I). The interesting result of the NQR measurements is the observation of a phase transition, occurring at $\approx 196\text{ K}$ and indicated by the sudden change of the sign of dv/dt , see Figure 9. It is very likely that this phase transition is of higher order, since there is no jump in the frequencies. The factum of two crystallographically independent iodines is preserved in the low temperature phase, too.

1,2-Diammoniummethane- and 1,3-Diammoniumpropane Halides

The temperature dependence of the ^{79}Br NQR spectrum of 1,2-diammoniummethane dibromide and 1,3-diammoniumpropane dibromide shows typical Bayer-type behaviour, that is increasing resonance frequencies with decreasing temperature. We do not know the crystal structure of 1,3-diammoniumpropane dibromide. NQR, however, shows that both compounds must crystallize with a centrosymmetric space group, and for 1,2-diammoniummethane dibromide the structure is known (monoclinic, $C2/m$, $Z = 2$) [21]. Since only frequencies are available and not asymme-

try parameters and nuclear quadrupole coupling constants, it is too speculative to attribute the large difference in $\nu(^{79}\text{Br})$ between 1,2-diammoniummethane dibromide and 1,3-diammoniumpropane dibromide to an alternation of the nuclear quadrupole interaction with alternating number of the CH_2 groups in the paraffin chain.

There must be a break in structure by going from the bromides to the iodides.

The ^{127}I NQR spectrum of 1,2-diammoniummethane diiodide, which was studied from the decomposition temperature down to 77 K , reveals two phase transitions in the range $390 \leq T/\text{K} \leq 420$, see Figs. 4 and 5. Each of the three phases, the one stable at room temperature (phase III), the one existent between 400 K and 404 K , and the one stable above 404 K , shows two ^{127}I NQR lines. Therefore there is only one crystallographically independent iodine in the unit cells of these three phases. (The transition $\nu_1(m = \pm 1/2 \leftrightarrow m = \pm 3/2)$ could not be followed up at temperatures below 150 K , most probably because of saturation). It is interesting to note that the high temperature phase I must belong to a tetragonal, hexagonal, or cubic space

Table 12. Interionic distances (in pm) and angles (in degree) of hydrogen bonds in organic ammonium bromides and iodides.

Compound	N...Br	N-H	N...Br	\angle N-H...Br	Ref.
Anilinium-bromide (phase I) ^a	332.8 348.0	98.3 114.6	234.5 234.2	179.2 172.0	[3]
Anilinium-bromide (phase II) ^a	332.2 332.2 334.4	103.2 104.2 104.2	233.8 229.1 235.6	158.7 170.0 157.9	[4]
o-Phenylene-diammonium dibromide	330.8 340.2 339.4		230 ^b 305 275	160 ^b 100 120	[15]
p-Phenylene-diammonium dibromide	333 338 341				[17]
Methyl-ammonium-bromide	395				[18]
Ethyl-ammonium-bromide	337 338		240 240	169 160	[19]
1,2-Di-ammonium-ethane dibromide	334 337 337				[21]
L-Arginine monohydro-bromide monohydrate	337.4 335.0 335.8 350.3 342.0 340.9 337.1 322.9				[22]
L-Cystine dihydro-bromide	328 342 341				[23]
L-Leucine hydro-bromide	336 332 338 ^c				[24]
L-Valine hydrobromide	340 335				[26]
Glycyl-l-alanine hydrobromide monohydrate	334.5 336.0 340.1	84.8 98.2 76.3	256.7 260.5 266.1	152.9 133.9 164.0	[27]
L-Cystine dihydro-bromide dihydrate	329.3 337.9 333 340 345				[28]
Disarcosine hydro-bromide	324 330 329 337 333 342 ^c				[29]
Piperazinium dibromide monohydrate	335.9 329.6 344.6 ^c	95.8 83.8 95.8	260.8 248.0 293.6	135.6 164.8 114.7	^d

^a Values from neutron diffraction. ^c No hydrogen bond.
^b Only estimated values. ^d This work.

Table 12 (continued)

Compound	N...I	N-H	N...I	\angle N-H...I	Ref.
Anilinium-iodide (phase I) ^a	353.5 359.6	97.5 107.3	256.0 252.9	178.2 172.7	[7]
Anilinium-iodide (phase II) ^a	351.8 352.3 352.2	103.8 103.0 102.1	253.9 249.8 256.5	157.0 173.0 155.8	[7]
o-Phenylene-diammonium diiodide	351.7 363.9 360.8				[16]
Trimethyl-ammonium-iodide	346				[20]
L-Leucine hydroiodide	354 352				[25]
Glycyl-l-alanine hydroiodide monohydrate	354.5 356.3 363.2	90.7 91.3 94.5	268.4 280.4 270.4	158.9 141.3 167.5	[27]
L-Glutamic acid hydroiodide	352.7 352.5	93 103	259 258	175 152	[30]
Piperazinium monoiodide	353.6 364.2 347.1 369.9	91.6 85.0 80.3 76.0	263.8 281.9 270.8 293.3	166.6 163.6 159.2 158.2	^d

group, because $\eta(^{127}\text{I})$ is zero. The two ^{127}I NQR transitions show a contrary temperature behaviour, and $e^2 q Q h^{-1} (^{127}\text{I})$ of phase III goes through a maximum at $T \approx 310$ K. This may be caused by librational motions of the NH_3 - and/or CH_2 groups of the cation.

The ^{127}I NQR spectrum of 1,3-diammonium-propane diiodide is also quite informative. The four observed transitions show two iodines in the asymmetric unit of the (unknown) unit cell, see Figure 6. Furthermore, at $T \approx 366$ K a phase transition occurs. The high temperature phase I must be centrosymmetric (only one iodine is in the asymmetric unit of the elementary cell). The phase transition is connected with a hysteresis, as seen from Figs. 6 and 7. The large difference in the nuclear quadrupole coupling constants of the two crystallographically independent iodines is most probably based on considerable asymmetry in the $\text{N}-\text{H}\dots\text{I}$ hydrogen bond system of this compound.

Acknowledgement

We are grateful to the 'Deutsche Forschungsgemeinschaft' for support of this work. We also thank Helge Bertling and Dirk Borchers for NQR measurements on the diammoniumalkyl halides.

- [1] J. Hartmann and Al. Weiss, *Ber. Bunsenges. Phys. Chem.* **91**, 1195 (1987).
- [2] W. Pies and Al. Weiss, *Bull. Chem. Soc. Japan* **51**, 1051 (1978).
- [3] G. Fecher, Al. Weiss, W. Joswig, and H. Fuess, *Z. Naturforsch.* **36 a**, 956 (1981).
- [4] G. Fecher, Al. Weiss, and G. Heger, *Z. Naturforsch.* **36 a**, 967 (1981).
- [5] B. P. Schweiss, H. Fuess, G. Fecher, and Al. Weiss, *Z. Naturforsch.* **38 a**, 350 (1983).
- [6] W. Pies, M. Schahbazi, and Al. Weiss, *Ber. Bunsenges. Phys. Chem.* **82**, 594 (1978).
- [7] G. Fecher and Al. Weiss, *Ber. Bunsenges. Phys. Chem.* **90**, 1 (1986).
- [8] G. Fecher and Al. Weiss, *Ber. Bunsenges. Phys. Chem.* **90**, 10 (1986).
- [9] R. B. Creel, H. R. Brooker, and R. G. Barnes, *J. Magn. Reson.* **41**, 146 (1980).
- [10] C. R  rat, *Acta Cryst.* **13**, 459 (1960).
- [11] L. Pauling, *The Nature of the Chemical Bond*, 3rd ed., Cornell University Press, Ithaca, N.Y. 1960.
- [12] H. Bayer, *Z. Physik* **130**, 227 (1951).
- [13] D. Borchers and Al. Weiss, *Ber. Bunsenges. Phys. Chem.* **91**, 1182 (1987).
- [14] D. Schwarzenbach, *J. Chem Phys.* **48**, 4134 (1968).
- [15] C. St  lhandske, *Acta Chem. Scand.* **26**, 3029 (1972).
- [16] K. Kozawa and T. Uchida, *Bull. Chem. Soc. Japan* **55**, 943 (1982).
- [17] Q. Won Choi, C. H. Koo, J. Suk Oh, and Chung Soo Yoo, *J. Korean Chem. Soc.* **9**, 178 (1965).
- [18] E. J. Gabe, *Acta Cryst.* **14**, 1296 (1961).
- [19] F. Jellinek, *Acta Cryst.* **11**, 626 (1958).
- [20] G. M. Sheldrick and W. S. Sheldrick, *Acta Cryst.* **B26**, 1334 (1970).
- [21] I. S  tofte, *Acta Chem. Scand.* **A30**, 309 (1976).
- [22] S. K. Mazumdar and R. Srinivasan, *Z. Krist.* **123**, 186 (1966).
- [23] J. Peterson, L. K. Steinrauf, and L. H. Jensen, *Acta Cryst.* **13**, 104 (1960).
- [24] E. Subramanian, *Acta Cryst.* **22**, 910 (1967).
- [25] M. O. Chaney, O. Seely, and L. K. Steinrauf, *Acta Cryst.* **B27**, 544 (1971).
- [26] R. Parthasarathy and R. Chandrasekaran, *Indian J. Pure Appl. Physics* **4**, 293 (1966).
- [27] A. K  hrer, S.-Q. Dou, and Al. Weiss, to be published.
- [28] R. E. Rosenfield Jr. and R. Parthasarathy, *Acta Cryst.* **B31**, 816 (1975).
- [29] S. C. Bhattacharyya and N. N. Saha, *J. Cryst. Mol. Struct.* **8**, 209 (1978).
- [30] A. Kirfel and F. Wallrafen, *Z. Krist.* **171**, 121 (1985).